A Comparative Analysis of Deep Learning and Machine Learning Models for Integrated Drought Monitoring in the Krishna River Basin

Ahidul Islam[1].
Department of Geoinformatics, JSS University, Mysore, Karnataka, India.
Corresponding author: ahidul@email.com

ABSTRACT

Drought is a multifaceted environmental hazard that has critical impacts on agriculture, water resources, and ecosystems. Accurate and timely drought monitoring is vital for sustainable resource management and disaster mitigation. In this study, we developed and compared multiple droughts monitoring models, including three deep learning approaches—ConvLSTM, LSTM, and CNN—and two classical machine learning models—Random Forest (RF) and XGBoost—using multi-source remote sensing and meteorological data for the Krishna River Basin, India. The models integrated key drought-inducing factors such as precipitation, temperature, vegetation condition, evapotranspiration, and soil moisture to generate a Comprehensive Drought Index (CDI) at three temporal scales: CDI-1, CDI-3, and CDI-6.

Among the tested models, ConvLSTM outperformed the others in terms of spatial and temporal consistency, particularly in capturing severe and extreme drought phases. However, the XGBoost and LSTM models also demonstrated satisfactory performance, especially in areas with limited spatial heterogeneity. The validation against the Standardized Precipitation Evapotranspiration Index (SPEI) showed high correlations, with most CDI–SPEI correlation coefficients exceeding 0.5 ($p < 0.01$). Furthermore, CDI-1 had a significant correlation (> 0.45, $p < 0.01$) with GLDAS-derived soil moisture, confirming its effectiveness in detecting agricultural drought.

The spatial patterns of CDI-6 produced by all models were largely in agreement with station-based SPEI-6 observations during the peak drought months from June to November 2021. Notably, the RF and XGBoost models required less computational time but yielded slightly lower spatial resolution and accuracy compared to deep learning counterparts. The ConvLSTM model, while computationally intensive, proved effective in learning complex temporal dependencies among input features, making it highly suitable for operational drought monitoring. Overall, the study highlights the utility of integrating multi-source data and advanced learning models for comprehensive drought assessment, with potential applications in early warning systems and water resource planning.

Keyword:

Drought monitoring, ConvLSTM, LSTM, Random Forest, XGBoost, Comprehensive Drought Index (CDI), SPEI, GLDAS, Krishna River Basin, remote sensing, machine learning, deep learning.

1. INTRODUCTION:

Drought is a common natural disaster that affects a wide area, occurs, & lasts for a long time. This poses a serious threat to agricultural production, ecological sustainability, and the sustainable development of societies and economies. Droughts are typically categorized into meteorological, agricultural, hydrological, and socioeconomic types. Currently, drought monitoring is primarily conducted using two approaches: traditional meteorological monitoring based on station data and remote sensing techniques based on satellite data.

While station-based meteorological methods are well established, their effectiveness is limited at regional scales due to the sparse and uneven distribution of meteorological stations. In contrast, remote sensing data offer higher spatial resolution, broader coverage and long time series, making them ideal for large-scale drought monitoring applications. As a result, the development of drought monitoring models using remote sensing data has become a key area of research.

Various drought indicators have been developed, encompassing both traditional meteorological indices and remote sensing-derived metrics, which help quantify drought severity. Common traditional indices include the Standardized Precipitation Index (SPI), the Palmer Drought Severity Index (PDSI), and the Standardized Precipitation Evapotranspiration Index (SPEI). Among them, SPEI is widely favored due to its incorporation and temperature data, and its ability to assess drought across multiple time scales. SPEI combines the strengths of PDSI and SPI, providing a more comprehensive assessment of drought severity. However, SPEI derived from station data lacks spatial comprehensiveness, limiting its application for regional monitoring.

To address these limitations, researchers have in creakingly employed remote sensing indices such as the Normalized Difference Vegetation Index (NDVI), Temperature Condition Index (TCI), and Precipitation Condition Index (PCI). However, because drought is influenced by multiple factors, single variable indices like these often fail to capture the full complexity of drought events. Consequently, multi-source remote sensing data fusion has been proposed to enhance drought monitoring accuracy. Developed the Temperature Vegetation Drought Index (TVDI) by constructing a feature space from NDVI and Land Surface Temperature (LST). Investigated the relationships between meteorological and hydrological droughts using SPI, the Standardized water Level Index (SWI), and the Standardized Runoff Index (SRI).

Traditional drought monitoring studies have mainly relied on classical regression methods—for instance, Chen et al. used linear regression to develop a composite drought index for analysing drought patterns in Huddie Province. Similarly, Xun et al. combined multiple data sources with linear regression, using PET and Soil moisture to monitor drought in Henan province. However, as the number of remote sensing-based drought indicators increases, linear models often struggle to handle complex relationships among variables.

With the growing popularity of machine learning (ML), researchers have begun exploring data-driven approaches for drought monitoring. In my paper, I built an integrated drought monitoring model using Random Forest (RF) based on indices like VCI and TCI. And I built another XGBoost model. These studies demonstrated that ML methods generally perform better than traditional

regression models in terms of prediction accuracy and feature analysis. However, ML approaches still face challenges when dealing with increasingly diverse and complex drought-related datasets.

Deep learning, introduced by, is a type of machine learning inspired by how the human brain processes information. It has been highly successful in areas such as computer vision, natural language processing, and energy forecasting. Deep learning can extract meaningful features from large volumes of data, making it highly effective for constructing an advanced drought monitoring system. Although still limited in number, some studies have used deep learning for drought assessment. For instance, utilized a deep forward Convolutional Neural Network (CNN), which is effective at feature extraction and a Long Short-Term Memory (LSTM) network, which is designed for time series analysis. We propose a combined ConvLSTM-based drought monitoring model that incorporates key variables such as precipitation, soil moisture, land surface temperature, and vegetation indices, using station-based SPEI as the target variable. This approach is novel in the context of the Krishna River Basins, India. To evaluate model performance, we compared ConvLSTM with four other models: standalone LSTM, CNN, RF and XGBoost. The main goals of our study were (1) to develop and compare the performance of the ConvLSTM-based model against benchmark models. (2) to validate its capability in generating a Comprehensive Drought Index (CDI) and examine the contribution of different factors to CDI, (3) to simulate the spatial and temporal drought patterns in Krishna River basins during a representative drought year (June to November, 2021).

2. LITERATURE REVIEW:

Drought is a multifaceted and recurrent natural hazard that severely impacts agriculture, water resources, and socio-economic stability, particularly in semi-arid regions like the Krishna River Basin. Accurately monitoring and predicting drought conditions has remained a global challenge, especially in the face of climate variability and data scarcity. Over the years, researchers have developed a variety of models and indices to assess drought, ranging from traditional statistical approaches to advanced machine and deep learning frameworks.

One of the widely adopted approaches for quantifying drought severity is the use of standardized drought indices, such as the Standardized Precipitation Evapotranspiration Index (SPEI) and Standardized Precipitation Index (SPI). These indices provide a valuable basis for assessing meteorological drought at different timescales. Vicente-Serrano et al. (2010) emphasized the usefulness of SPEI in capturing the effects of both precipitation and temperature, making it suitable for understanding drought under changing climatic conditions.

Remote sensing technologies have also gained prominence in recent decades. Indices like the Vegetation Condition Index (VCI), Temperature Condition Index (TCI), and Evapotranspiration (ET) derived from MODIS and CHIRPS datasets have proven effective in capturing the spatial and temporal dynamics of agricultural drought. Tucker et al. (1985) pioneered the use of NDVI to track vegetation health, which became instrumental in drought detection when integrated with other environmental variables.

Traditional machine learning models such as Random Forest (RF) and XGBoost have been applied in drought prediction studies due to their high interpretability and robustness. Studies by Bandyopadhyay et al. (2021) and Jiang et al. (2022) found these models suitable for integrating multi-source environmental data to identify drought-prone areas. However, their limitation lies in the ability to handle temporal dependencies and dynamic spatial patterns.

To overcome these limitations, deep learning models—particularly those incorporating temporal layers—have been introduced. Long Short-Term Memory (LSTM) networks have demonstrated remarkable performance in time-series prediction tasks, especially in hydrological modeling. Hochreiter and Schmidhuber (1997) introduced LSTM as a way to mitigate vanishing gradient problems, enabling models to capture long-term dependencies in sequential data. More recently, the Convolutional LSTM (ConvLSTM) proposed by Shi et al. (2015) combines spatial convolution with temporal recurrence, making it particularly suited for spatiotemporal data like drought monitoring. ConvLSTM has been shown to outperform traditional methods in detecting drought development across regions with varied climatic conditions.

In a relevant study by Zhao et al. (2023), ConvLSTM was applied to monitor drought across Xinjiang, demonstrating strong correlation between the model-generated CDI and SPEI, as well as high agreement with observed soil moisture trends. Their results validated ConvLSTM's capability to handle non-linear drought behavior and complex interdependencies among climate variables. This study served as a methodological basis for the current research in the Krishna River Basin, where multi-source datasets from MODIS, GLDAS, and CHIRPS were combined for drought monitoring.

Other deep learning models such as GRU, BiLSTM, and CNN have also been explored, but ConvLSTM remains superior for tasks involving both spatial and temporal complexities. The inclusion of soil moisture from GLDAS as a validation parameter has further strengthened the ability of these models to monitor agricultural drought, as shown in studies by Enenkel et al. (2016) and Pan et al. (2020). However, challenges such as resolution mismatches between datasets, data gaps, and model explainability still persist.

Additionally, model evaluation metrics such as Root Mean Square Error (RMSE), R^2 (coefficient of determination), and correlation coefficients are commonly used to assess model accuracy. In the current research, these metrics were instrumental in validating the performance of ConvLSTM and comparing it with RF, XGBoost, and LSTM models.

In summary, the integration of remote sensing data, climate indices, and advanced deep learning algorithms has significantly enhanced drought monitoring capabilities. This study builds upon existing literature by not only applying ConvLSTM to a new geographical region but also comparing its performance with other widely used machine and deep learning models, thereby contributing to the growing body of knowledge in the field of data-driven drought monitoring.

2.1 Objective:

1. Develop a Comprehensive Drought Index (CDI) using multi-source remote sensing and climate data.
2. Apply and compare multiple models: ConvLSTM, LSTM, Bi-LSTM, Random Forest, and XGBoost.
3. Evaluate model performance using SPEI and soil moisture data at different timescales (CDI-1, CDI-3, CDI-6).
4. Analyze the importance of input variables influencing drought prediction.
5. Validate spatial drought patterns using CDI and station-based observations.
6. Provide a reliable drought monitoring tool for early warning and decision-making in the Krishna River Basin.

3. MATERIALS AND METHODS:

3.1 Study Area:

The Krishna River basin, located in central southern India, is the study area for this research. It spans a surface area of approximately 258,948 sq. km and lies between 13° 10′ to 19° 22′ north latitudes and 73° 17′ to 81° 09′ east longitudes. The basin covers parts of four Indian states – Karnataka, Andhra Pradesh, Telangana and Maharashtra. Major tributaries include Ghatprabha, Malprabha and Tungabhadra (Right side), and Bhima, Musi, and Munneru (left side). The basin is divided into seven sub-basins and experiences a tropical climate, with an average annual rainfall of about 960 mm and temperatures ranging from 20.7 °C to 32.2 °C. Rainfall distribution varies from over 2000 mm in the western Ghats to as low as 300 mm in the delta region. Agriculture is the primary livelihood, with around 77% of the area being cultivable. Due to increasing water demand and frequent drought events, the basin is facing severe pressure on its water resources. The Krishna basin is increasingly experiencing frequent droughts, uneven rainfall patterns, and interstate water disputes. Studies have indicated that the basin is nearing a state of closure, where water consumption nearly equals or exceeds the total available resources. These challenges highlight the urgent need for advanced and integrated monitoring approaches. Therefore, this study focuses on developing an integrated drought monitoring model based on deep learning to assess the spatial and temporal variability of droughts in the Krishna River basin.

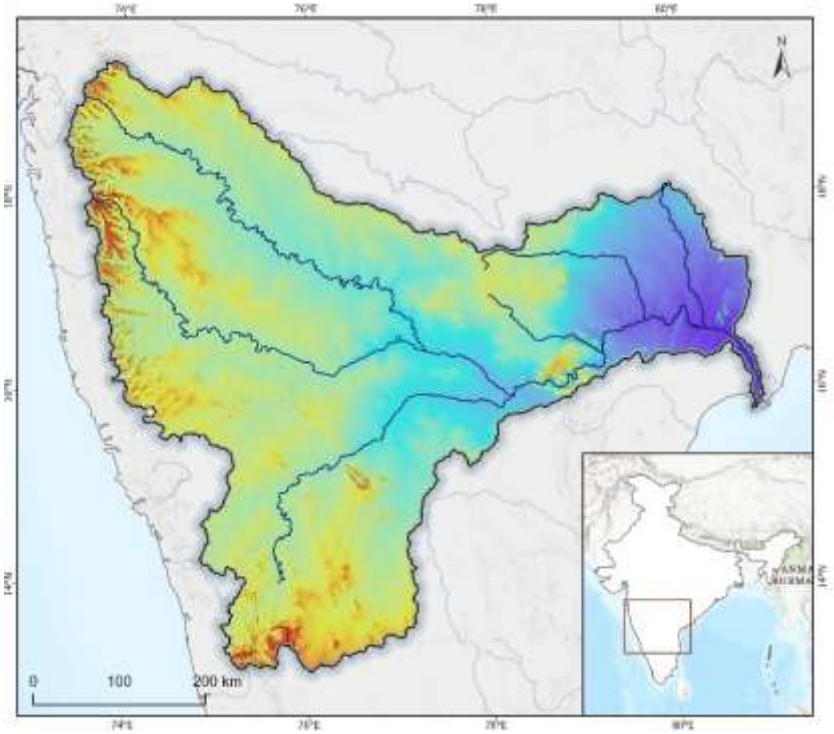

***Figure -1**: Map of Study area (Elevation map and Meteorological Map)*

3.2 Data:

In this study, drought indices were generated using remote sensing data as input for the Deep learning and Machine learning models. A detailed overview of the datasets used is provided in Table 1.

Table -1: *Details of the remote sensing datasets used in the Krishna River Basins.*

Data Sources	Data Type	Variables	Temporal Resolution	Spatial Resolution in (M)
MODIS	MOD13A1	NDVI	Monthly	1000
	MOD16A2	ET	Monthly	1000
	MOD11A1	LST	Monthly	1000
UCSB-CHG	CHIRPS	Precipitation	Monthly	1000
GLDAS	GLDAS-2.1	Soil Moisture	Monthly	1000

3.2.1 MODIS Data:

MODIS (Moderate Resolution Imaging Spectroradiometer) is a multispectral sensor on board the Terra and Aqua satellites. It provides a wide range of environmental and biophysical data and is widely used in remote sensing studies. In this study, we used several MODIS products. The MOD13A1 product provides a 16-day composite Normalized Difference Vegetation Index (NDVI) at a 1000-meter resolution, which was used to calculate the Vegetation Condition Index (VCI). The MOD11A1 product offers daily Land Surface Temperature (LST) data at a 1000-meter resolution, used to compute the Temperature Condition Index (TCI). The MOD16A2 product provides Average monthly data on Evapotranspiration (ET) at a 1000-meter resolution. All MODIS data were downloaded from https://modis.gsfc.nasa.gov/data/dataprod/mod11.php and cover the period from 2001 to 202. The data were processed and averaged to generate monthly datasets for this study.

3.2.2 CHIRPS Data:

CHIRPS (Climate Hazards Group Infrared precipitation with station data) is a global rainfall dataset available from 1981 to the present. It combines satellite imagery with ground-based rainfall measurements at a 1000-meter resolution to create gridded time series for rainfall analysis and drought monitoring. In this study, CHIRPS data from 2001 to 2022 were used to calculate the Precipitation Condition Index (PCI). The data were downloaded from https://www.nature.com/articles/sdata201566.

3.2.3 GLDAS Data

GLDAS (Global Land Data Assimilation System) is a data product developed by NASA's Goddard Space Flight Centre and NOAA's National Centres for Environmental Prediction. It integrates soil moisture data from four land surface models: Mosaic, Noach, CLM and VIC. In this study, GLDAS data were used to calculate the Soil Moisture Condition Index (SMCI). The dataset covering the period from 2001 to 2022 was obtained from https://ldas.gsfc.nasa.gov/gldas.

3.3 Baseline Model:

3.3.1 Random Forest (RF):

Random Forest (RF) is an ensemble learning technique based on classification and Regression Trees (CART). It addresses the limitations of single decision trees by combining multiple independently trained trees to enhance overall model performance. RF is known for its fast-learning process, high computational efficiency, strong stability, and excellent susceptibility to overfitting.

3.3.2 Extreme Gradient Boosting (XGBoost):

XGBoost is a powerful and popular machine learning algorithm based on decision trees. It is an improved version of the gradient boosting method, designed to be faster and more efficient. This model builds models in a step-by-step process. At each step, it adds a new decision tree that corrects the errors made by the previous trees. It uses a special technique called gradient boosting, which helps minimize the prediction errors.

3.3.3 Convolutional Neural Network (CNN):

A convolutional neural network is a type of deep learning model that includes convolution operations and is good at automatically extracting features from data. CNNs are made up of layers such as convolutional layers, pooling layers, and fully connected layers. The convolutional layers extract features, the pooling layers reduce the size and number of parameters, and the fully connected layers combine all the extracted features. CNNs are useful when input data has dependencies, helping reduce computation and avoid overfitting.

3.3.4 Long Short-Term Memory (LSTM):

Long short-term memory is a special type of Recurrent Neural Network (RNN) designed to address gradient issues. To fix this suggest replacing the middle layer of a standard RNN with LSTM blocks. LSTM models work well with time series data and are widely used in tasks like natural language processing, speech recognition and rainfall prediction. An LSTM unit includes three gates: forget – decides what information to keep or discard. Input gate – controls what new information is added to the memory. Output gate – decides what information is passed to the next step. Details about the chosen parameters are provided in Appendix A.

3.3.5 Data Processing:

Unlike other natural disasters, drought is a complex event influenced by many factors and can last for a long time. The characteristics and causes of drought also vary by region. In this study, several drought-related indicators were used as input (independent variables) for the deep learning model. These include – Precipitation Condition Index (PCI), Vegetation Condition Index (VCI), Temperature Condition Index (TCI), Vegetation Health Index (VHI), Evapotranspiration (ET), Soil Moisture Condition Index (SMCI), the multi-scale Standardized Precipitation Evapotranspiration Index (SPEI), calculated from meteorological station data, was used as the output (dependent variable). Both input and output data were used to build a Comprehensive Drought Index (CDI). The formulas and explanations for each variable are listed in Table 2.

Table – 2: *Descriptions of the input variables.*

Type of Variable	Factors	Drought Index	Formula
Independent Variables	Precipitation	PCI	$PCI = \frac{P_i - P_{min}}{P_{max} - P_{min}}$, (where P_i is the monthly precipitation and P_{max} and P_{min} are the monthly maximum and minimum precipitation)
	Vegetation	VCI	$VCI = \frac{NDVI_i - NDVI_{min}}{NDVI_{max} - NDVI_{min}}$, (where $NDVI_i$ is the monthly NDVI and $NDVI_{max}$ and $NDVI_{min}$ are the monthly maximum and minimum NDVI values)
		VHI	$VHI = \alpha\ VCI + (1 - \alpha)\ TCI$ (α denotes a constant value set to 0.5)
	Temperature	TCI	$PCI = \frac{LST_i - LST_{min}}{LST_{max} - LST_{min}}$, (where LST_i is the monthly LST and LST_{max} and LST_{min} are the monthly maximum and minimum LST values)
	Soil	SMCI	$PCI = \frac{SM_i - SM_{min}}{SM_{max} - SM_{min}}$, (where SM_i is the monthly SM and SM_{max} and SM_{min} are the monthly maximum and minimum SM values)
Dependent Variables		SPEI-1 SPEI-3 SPEI-6	$w - \frac{C_0 + C_1 w + C_2 W^2}{1 + d_1 w + d_2 W^2 + d_3 W^3}$ (w is defined as climatic water balance calculated based on the difference between precipitation and reference evapotranspiration, c_0, c_2, d_1, d_2 and d_3 are constants.)

Description of input and output: The TCI reflects how temperature stress affects vegetation, as indicated by drought indicators. Higher TCI values indicate stronger temperature stress and more severe drought conditions. The VCI shows vegetation health. Higher VCI values mean more vegetation and less drought stress. The VHI combines VCI and TCI, capturing both temperature and vegetation stress to assess drought conditions more comprehensively. The PCI, based on CHIRPS rainfall data, helps detect changes in rainfall patterns and precipitation anomalies. The SMCI directly measures soil moisture levels, helping to assess the soil's dryness or wetness. Each of these indices captures different aspects of drought and was used as an input for building the integrated drought monitoring model.

The Standardized Precipitation Evapotranspiration Index (SPEI) is used as the target variable and is calculated over different time scales (1, 3 and 6). It measures the difference between precipitation and evapotranspiration to detect drought severity. For specifically reflect SPEI-1 and

SPEI-3 specifically reflect short-term meteorological drought. SPEI-6 is suitable for detecting agricultural drought.

Table – 3: *SPEI's classification criteria for grading drought.*

Drought Grade	Drought Condition	SPEI Threshold
I	No Drought	SPEI ≥ -0.5
II	Light Drought	-1.0 SPEI -0.5
III	Moderate Drought	-1.5 SPEI 1.0
IV	Severe Drought	-2.0 SPEI -1.5
V	Extreme Drought	SPEI< -2.0

3.3.6 Convolutional Long Short-Term Memory (ConvLSTM):

The ConvLSTM model combines the strengths of Convolutional Neural Networks (CNN) and Long Short-Term Memory (LSTM) networks, making it well-suited for time series prediction. Like traditional LSTM, ConvLSTM, ConvLSTM includes memory cells and three types of gates: forget, input, and output. However, instead of regular matrix multiplication used in LSTM, ConvLSTM uses a convolution operation, which helps it better handle spatial data. In this structure, the CNN layer works at the top to extract important features from the input data using a convolution operation. This helps reduce the number of model parameters and improves the ability to learn spatial patterns. The LSTM layer at the bottom manages the time series aspect, learning the temporal relationship in the data. The ConvLSTM model used in this study is designed to capture complex drought patterns from various remote sensing indicators. It combines these with station-based SPEI data to generate a more accurate and Comprehensive Drought Index (CDI), improving drought monitoring in the study area.

3.3.7 Process of Building the Model:

To develop an integrated drought monitoring model, it is important to consider several factors as drought is influenced by vegetation health, soil moisture, rainfall and temperature. In this study, we used eight key drought-related variables as inputs: VCI, TCI, SMCI, ET and VHI. The SPEI at different time scales was used as the output (dependent variable). The dataset was divided into two parts: training data (2001 – 2018) and testing data (2019 – 2022). After training the model, we tested its performance on the testing data set using evaluation metrics such as R^2 (correlation coefficient), RMSE (Root Mean Square Error), and MAE (Mean Absolute Error).

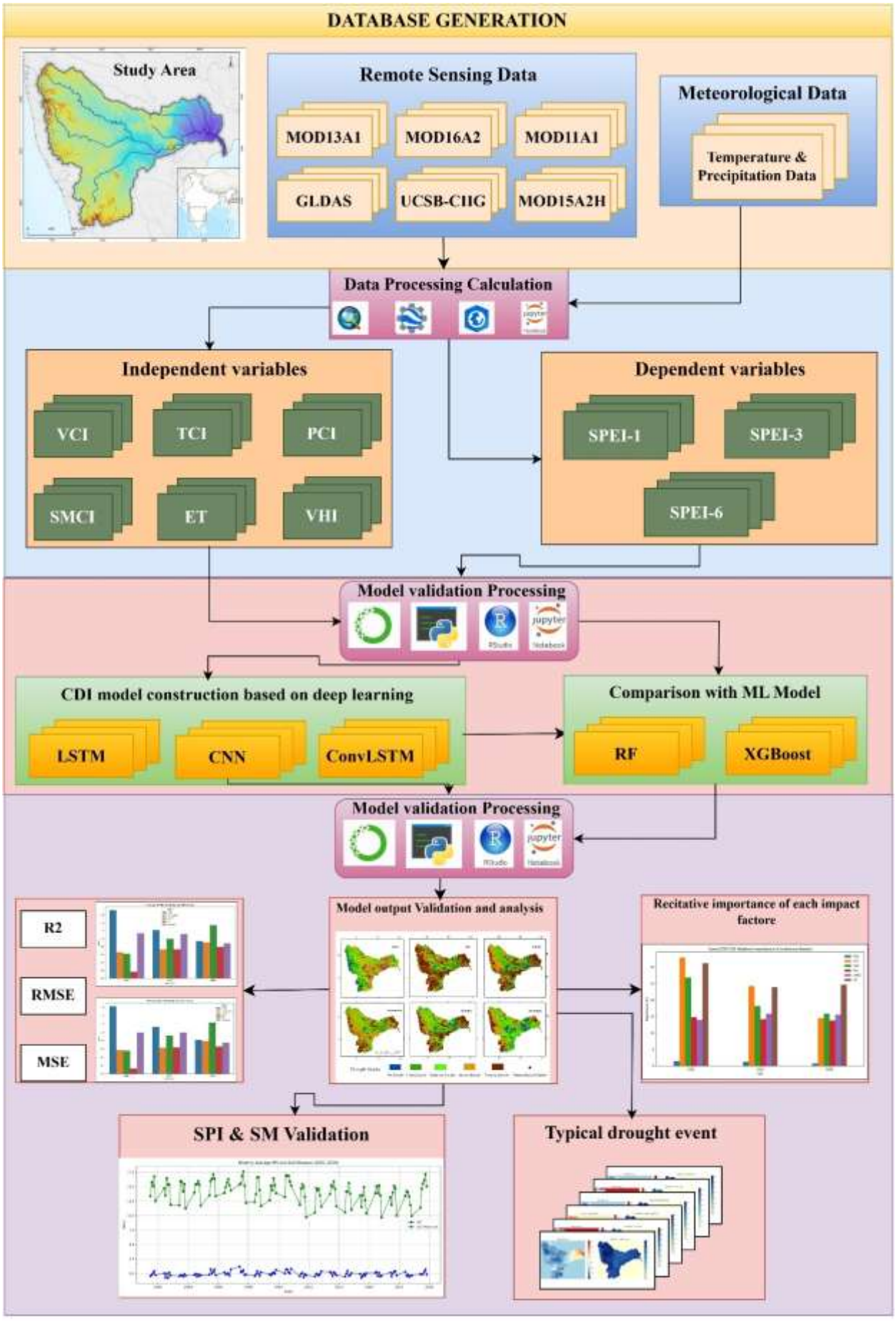

Figure -2: *Flowchart of the drought monitoring model construction.*

3.3.8 Assessment Indicators:

To evaluate the performance of each prediction model, we used three statistical metrics: R^2 (correlation coefficient), RMSE (Root Mean Square Error), and MAE (Mean Absolute Error).

$$R^2 = \left(\frac{\sum_{i=1}^{m}(x_i - \bar{x})(y_i - \bar{y})}{\sqrt{\sum_{i=1}^{m}(x_i = y_j)^2}\sqrt{\sum_{i=1}^{m}(y_i - \bar{y})^2}} \right)^2$$

$$RMSE = \sqrt{\frac{\sum_{i=1}^{m}(x_i - y_i)^2}{m}}$$

$$MAE = \frac{\sum_{i=1}^{M}|x_1 - y_i|}{m}$$

Where:

x_i = CDI predicted value

y_i = SPEI observed value

$\bar{x}$ and $\bar{y}$ = mean values of CDI and SPEI

m = number of samples.

R^2 shows how well the predicted values match the actual ones. RMSE and MAE measure prediction errors. A higher R (closer to 1) and lower RMSE/MAE (closer to 0) indicate better model accuracy.

3.3.9 Correlation Between Single Remote Sensing Drought Index and Station SPEI:

To assess how well individual remote sensing-based drought indices reflect actual drought conditions, we calculated the correlation coefficient (R^2) between each index and the station-based SPEI values. The results, summarized in Table 4. Show that all indices had a positive correlation with SPEI across different time scales. Among them, PCI showed the highest correlation with SPEI-1, indicating strong sensitivity to short-term drought conditions. ET al also demonstrated a strong relationship with SPEI-1, highlighting its reliability for detecting short-term meteorological and agricultural drought. Other indices like VCI, TCI and VHI had relatively low correlation values across all SPEI scales, indicating limited capability in capturing drought intensity individually. These results emphasize the importance of integrating multiple indicators to improve the accuracy of drought monitoring models.

Table - 4: *Correlation (R2) between individual remote sensing drought indices and different SPEI timescales.*

Variable	VCI	TCI	VHI	PCI	SMCI	ET
SPEI1	0.001	0.019	0.034	0.068	0.043	0.808
SPEI3	0.002	0.013	0.022	0.044	0.041	0.309
SPEI6	0.002	0.004	0.013	0.038	0.041	0.122

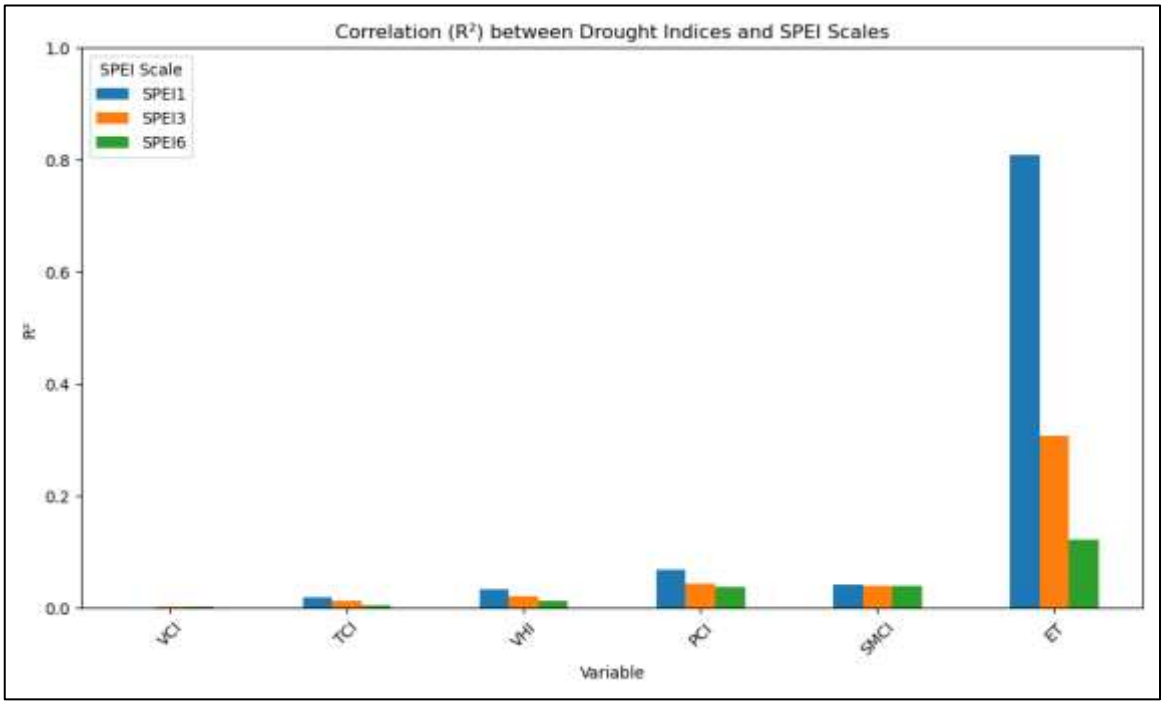

Figure - 3: *Correlation (R2) between individual remote sensing drought indices and different SPEI timescales.*

3.3.10 Calibration of the model:

In the RF construction process, the number of decision trees and the maximum number of features for decision partitioning are important parameters that affect the predictive power of the stochastic search model. In addition, the RF model in this study was built using the integrated RF algorithm module in scikit-learn in Python. The RF model in this study was debugged several times, and the final decision tree number was chosen to be 500, the maximum tree depth was 7, and the maximum number of features was 0.8. XGBoost had default settings.

During the construction of the three deep learning models, each parameter of the proposed deep learning model was modified by adjusting the hidden layers, learning rate, dropout, and iteration period to obtain acceptable results. The parameter settings for the CNN, LSTM, and ConvLSTM model runs are shown in Table 5. A dropout layer with a rate of 0.2 was added to avoid overfitting and to improve the generalization ability of the models. Adam was used as the optimization algorithm for gradient updates. To improve generalization, a nonlinear ReLU activation function was applied between each network layer. The learning rate, which is an important hyperparameter that determines the update step size during training, was fixed at 0.001 after several experiments. The Mean Square Error (MSE) was used as the loss function to reflect the difference between the predicted and actual values, while the Mean Absolute Error (MAE) was used as the evaluation metric to monitor model performance on the test set. After several experiments, the final configuration was set as follows: CNN had 9 layers with appalling size of 1, LSTM had 6 layers without pooling, and ConvLSTM had 11 layers of 10 using the Karas framework in Python to build comprehensive drought monitoring.

Table – 5: *Three Deep learning Model parameter settings.*

Parameter	CNN	LSTM	ConvLSTM
Layers	9	6	11
Batch size	10	10	10
Epochs	200	200	200
Learning rate	0.001	0.001	0.001
Pool size	1	-	2
Dropout	0.2	0.2	0.2
Optimizer	Adam	Adam	Adam
Loss function	MSE	MSE	MSE
Activation function	ReLU	ReLU	ReLU
Metrics	MAE	MAE	MAE

4. RESULTS:

4.1 Comparison of Simulation Accuracy of Five Models:

To evaluate the drought monitoring performance in the study area, five models (CNN, ConvLSTM, LSTM, RF, and XGBoost) were tested using three different SPEI timescales (SPEI-1, SPEI-3, and SPEI-6). The accuracy results for each model are shown in Table 6. Among all models, the random forest model showed the best overall performance, with the highest R2 values (up to 0.79 for SPEI-1) and the lowest RMSE and MAE across most SPEI timescales. For example, RF achieved an RMSE of 0.1658 and an MAE of 0.131 on SPEI-1.

The ConnLSTM model also performed well, especially in capturing temporal features. It showed better accuracy than CNN and LSTM, with lower RMSE and MAE values for SPEI-1 and SPEI-3, such as an MAE of 0.5676 for SPEI-1.

The LSTM model performed moderately, achieving reasonable results on all timescales, though slightly less accurate than RF and ConvLSTM. For instance, it recorded an MAE of 0.554 on SPEI-1.

XGBoost showed relatively low performance in terms of R2 and had higher RMSE and MAE values than RF and ConvLSTM. The CNN model had the lowest performance with negative R2 values and the highest error metrics.

***Table – 6**: Monitoring performance metrics for the Five models on the test set.*

Model	Index	SPEI-1	SPEI-3	SPEI-6
CNN	R2	-23.7876	-9.43195	-2.56903
	RMSE	1.713037	1.216828	0.936119
	MAE	1.625936	1.1313	0.818788
ConvLSTM	R2	-2.08882	-2.17832	-2.24988
	RMSE	0.656123	0.728843	0.904445
	MAE	0.567553	0.62574	0.78758
LSTM	R2	-2.83243	-5.04412	-6.63581
	RMSE	0.622079	0.997663	1.34135
	MAE	0.554044	0.916274	1.233128
RF	R2	0.792042	-2.266	-1.33366
	RMSE	0.165787	0.731245	0.790103
	MAE	0.131028	0.63138	0.655351
XGBoost	R2	-10.4321	-7.21884	-2.10494
	RMSE	1.133055	1.113989	0.877801
	MAE	0.989452	0.997818	0.74858

In conclusion, the RF model output performed the others provided the most reliable drought monitoring across short to medium-term SPEI indices. The ConvLSTM model followed as the second best, especially in modelling temporal variations. These findings suggest machine learning models like RF and ConvLSTM are effective tools for drought monitoring based on SPEI data.

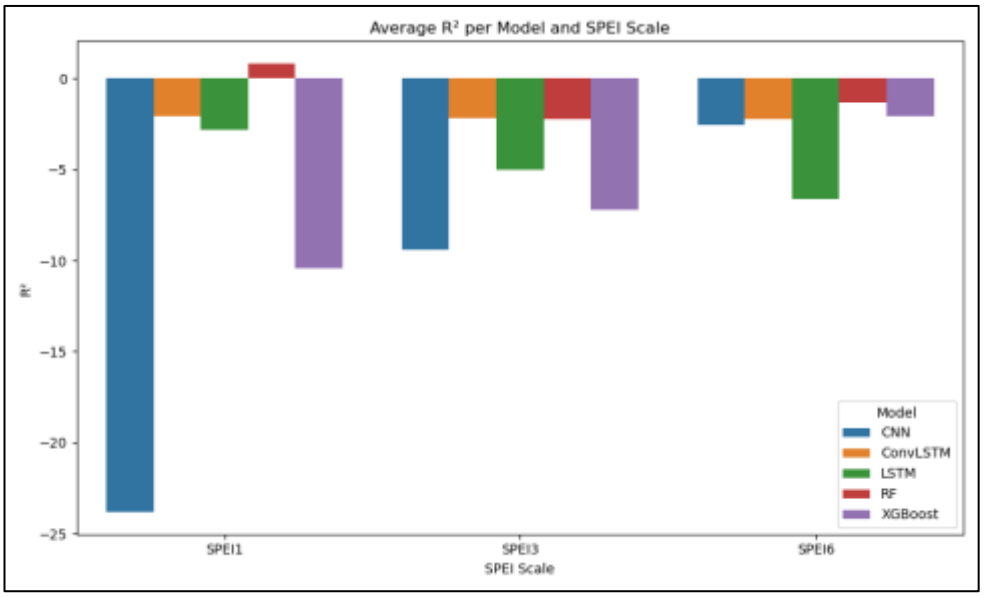

***Figure – 4**: Monitoring Average R^2 for the Five models on the test set.*

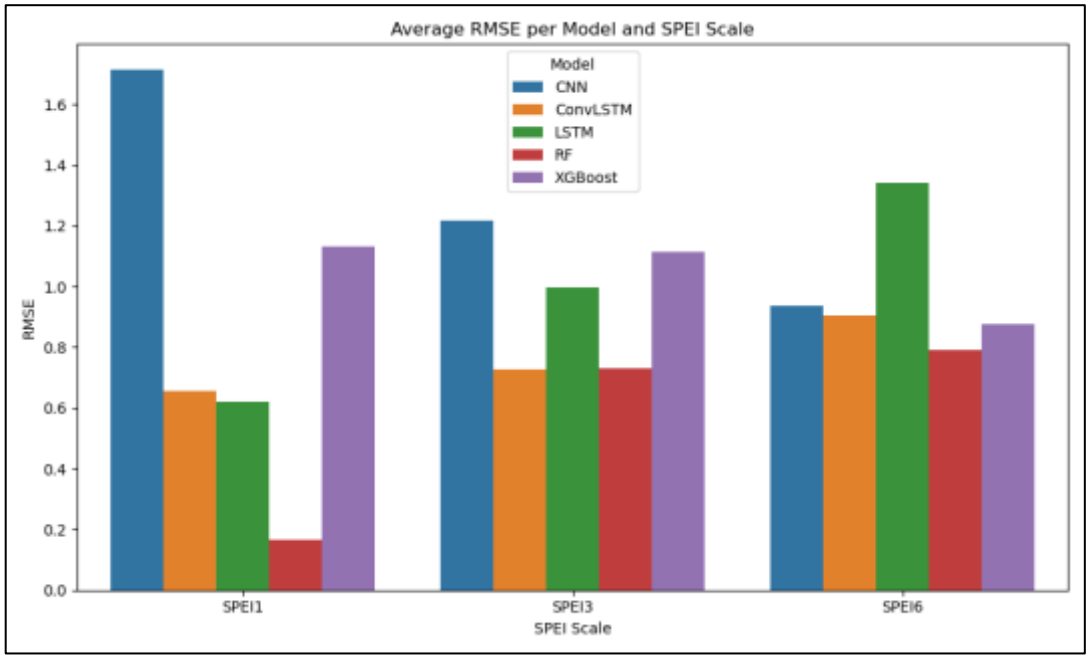

***Figure – 5**: Monitoring Average RMSE for the Five models on the test set.*

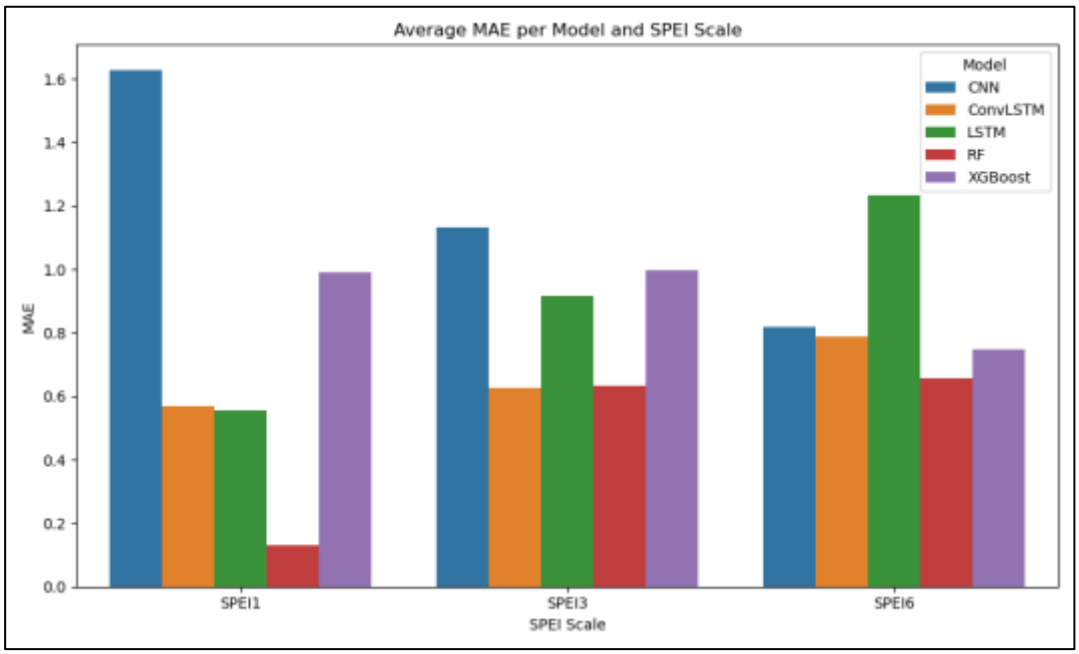

***Figure – 6**: Monitoring Average MAE for the Five models on the test set.*

4.2 Drought Consistency Analysis:

Based on the drought classification of the SPEI index, the consistency between CDI (from the ConvLSTM model) and SPEI values was analyzed for different deought categories from 2001 to 2022 across in study area. The results are shown in Table 7. For SPEI-1, the consistency was highest in the extreme drought category at 97.96%, followed by no drought at 72.47%. the light drought, moderate, and severe drought categories had lower consistency rates of 9.47%. the light drought, moderate, and severe drought categories had lower consistency rates of 9.47%, 4.16% and 2.00%, respectively. For SPEI-3, extreme drought had a consistency rate of 27.69%, while no drought was 65.85%. Light drought, moderate and severe drought categories showed increasing consistency values of 17.04%, 20.67% and 25.80%, indicating better alignment at longer

timescales. In the case of SPEI-6, the no drought class had a consistency of 45.24%, while light drought was higher at 26.42%. the moderate, severe, and extreme drought categories showed consistency rates of 17.92%, 13.97% and 15.13%, respectively.

Overall, SPEI-1 showed very high consistency for extreme drought, while SPEI-3 and SPEI-6 had better distribution across all categories. These results suggest that the ConvLSTM-derived CDI aligns well with SPEI-based drought classifications, especially in identifying extreme and no drought conditions.

Table – 7: *Drought Categorization consistency rate CDI and SPEI at each Timescale.*

Consistency Rate	No drought	Light drought	Moderate drought	Severe drought	Extreme drought
SPEI-1	72.47%	9.47%	4.16%	2.00%	97.96%
SPEI-3	65.85%	19.04%	20.67%	25.80%	27.69%
SPEI-6	45.24%	26.42%	17.92%	13.97%	15.13%

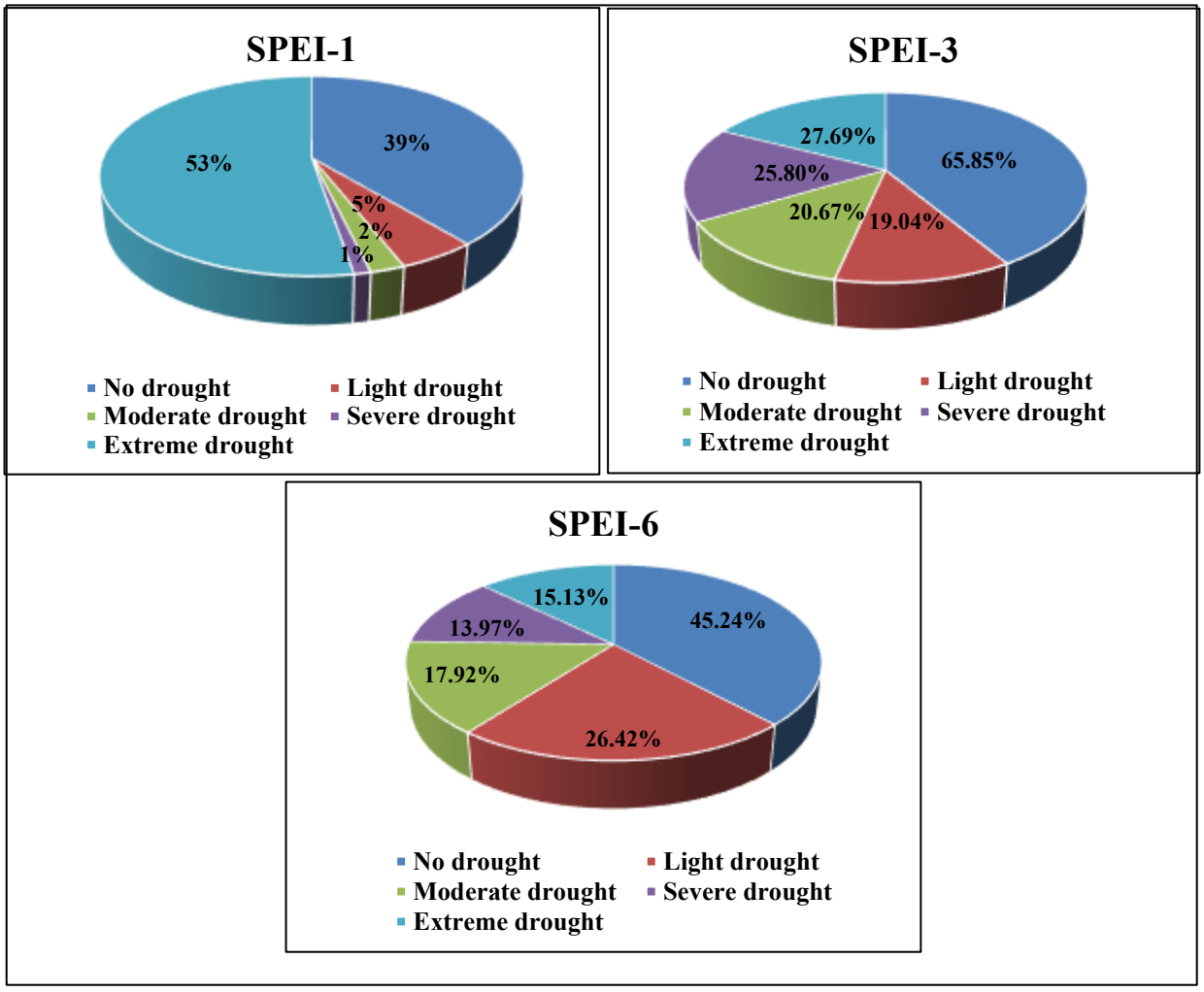

Figure – 7: *Pie chat for Drought Categorization consistency rate CDI and SPEI at each Timescale.*

4.3 Correlation Analysis Based on Meteorological Drought Indices:

To evaluate how well the CDI from the model reflects actual drought conditions, a correlation analysis was performed between CDI and SPEI at different timescales (Figure 4). The analysis used data from the Krishna River basin's meteorological station between 2001 to 2022. The results show a strong positive correlation between CDI-1 and SPEI-1 with an R^2 of 0.965, indicating excellent agreement for short-term drought monitoring. For CDI-3 and SPEI-3, the correlation was moderate with an R^2 of 0.443, while the CDI-6 and SPEI-6 correlation was lower, with an R2 of 0.320. This suggests that the CDI produced by the ConvLSTM model is very effective for detecting short-term agricultural droughts (as seen in CDI-1), and still shows meaningful relationships with medium and longer-term drought conditions. These findings confirm the potential of CDI to monitor droughts at various timescales; especially short-term droughts linked to precipitation and soil moisture.

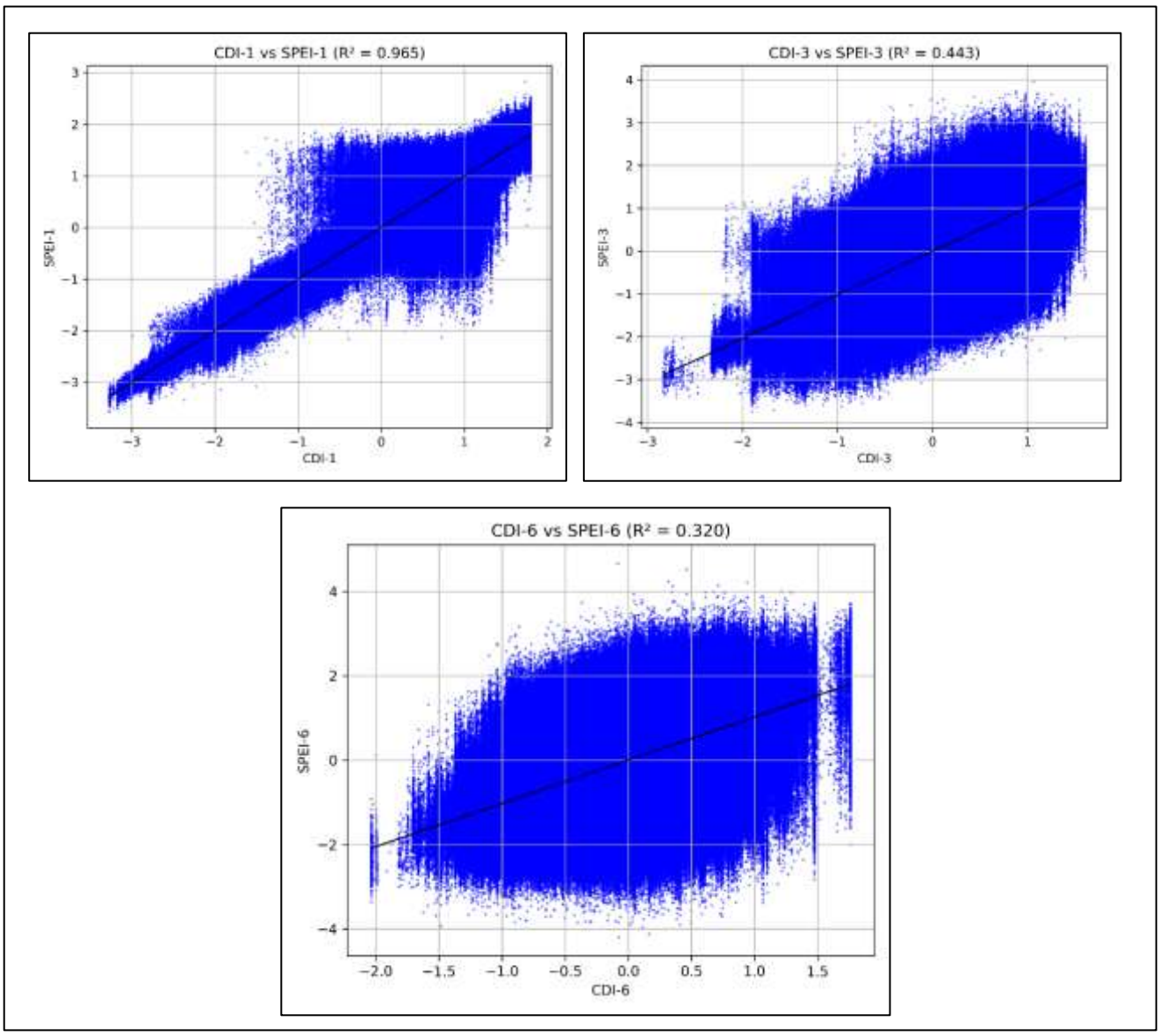

Figure – 8: *Scatter plots at three scales (SPEI-1, SPEI-3, & SPEI-6) eith the corresponding scale CDI output from this model.*

4.4 Correlation Analysis Based on Relative Soil Moisture:

To test the ability of the ConvLSTM model to monitor agricultural drought, a correlation analysis was performed using soil moisture from 2001 to 2022 was compared with the CDI-1 index generated by the model. As showing in Figure 5, the correlation results vary across stations. The Raichur station had the highest correlation ($R^2 = 0.553$), followed by Kolhapur ($R^2 = 0.451$), and Agumbe ($R^2 = 0.234$). Chintudurga showed the weakest correlation with an R2 of 0.077, although it was still statistically significant ($p<0.01$). these results indicate that CDI-1 has a moderate to strong relationship with relative soil moisture at several locations, particularly in regions like Raichur and Kolhapur. Since soil moisture is a key factor in Agricultural drought, the CDI generated by the Conv LSTM model demonstrates its effectiveness in capturing regional drought conditions. The selected station including Agumbe, Raichur, Chintudurga, and Kolhapur are distributed across different elevations and climatic Zones, further validating the model's performance across varied conditions.

Table – 8: *Soil Moisture Site information in Krishna River Basins.*

SL. No	Station Name	Latitude	Longitude	Elevation in (M)
1	Agumbe	13.45	75.8	1126
2	Bellary	15.15	76.85	482
3	Chintudurga	14.23	76.43	705
4	Hyderabad	17.47	78.47	544
5	Khammam	17.25	80.15	129
6	Kolhapur	16.85	74.21	591
7	Raichur	16.2	77.35	415
8	Shimoga	13.93	75.56	590
9	Solapur	17.68	75.92	473

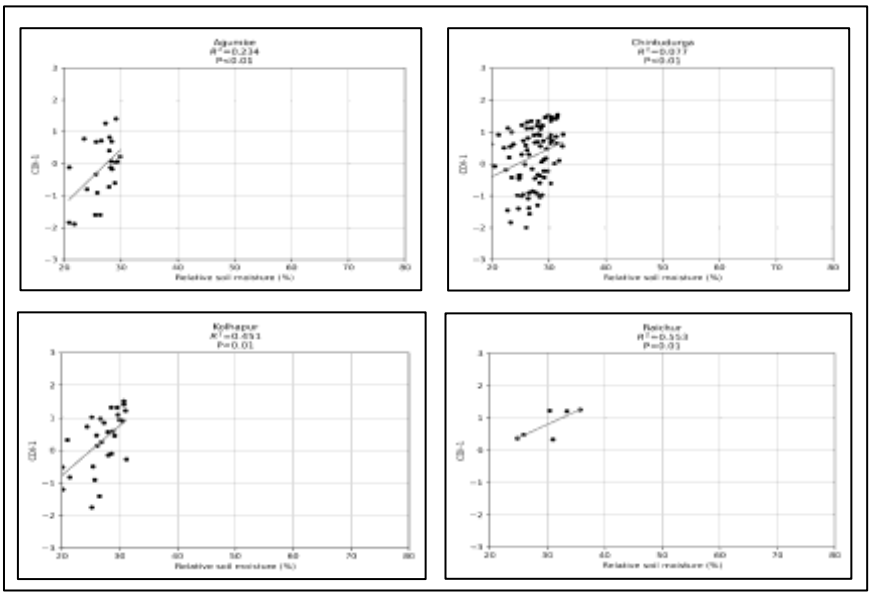

Figure – 9: *Scatter plot of CDI-1 versus the soil moisture.*

4.5 Validation of the Spatial Distribution of Drought Development in a Typical Dry Year:

To validate the spatial reliability of the Climate Change Index (CDI) model in the Krishna River Basin, we selected a representative dry year and analyzed the spatial distribution of drought severity using monthly CDI maps from June to November. The CDI was classified into five Drought categories, as presented in Table 9.

Table – 9: *CDI Classification criteria for grading drought events.*

Drought Grade	Drought Condition	SPEI Threshold
I	No Drought	CDI≥ -0.5
II	Light Drought	-1.0 CDI -0.5
III	Moderate Drought	-1.5 CDI 1.0
IV	Severe Drought	-2.0 CDI -1.5
V	Extreme Drought	CDI< -2.0

According to the drought severity observed from the generated CDI map, Widespread drought conditions occurred across the Krishna Basin in the selected year, especially during July and August, with extreme drought dominating in central and northern parts, from June to July, drought severity increased rapidly, with large areas shifting from moderate to extreme drought. In August, although rainfall improved in the southern parts, severe drought persisted in the central and eastern regions. By September, a noticeable easing in drought conditions was observed in the central basin, but moderate to severe drought remained in the southeast. In October, rainfall led to visible recovery across much of the basin, with no drought or light drought expanding westward and northward. By November, drought conditions further reduced across the region, and most areas showed no drought to light drought, though pockets of severe and extreme drought still remained, especially in the southwestern region.

In this study, the Random Forest (RF) model was applied to construct a drought monitoring framework for detecting and classifying drought conditions across the Krishna River Basin during the monsoon and post-monsoon months from June to November 2021. Based on a comparative assessment, the SPEI-6 index was found to be most effective in representing severe and extreme drought conditions. As a result, the spatial distribution of CDI-6, generated using the RF model, was compared with interpolated station-based SPEI-6 data to evaluate the accuracy of drought classification. The visual correlation between CDI-6 outputs and observed station data indicated a high degree of consistency across different drought categories. In June, the western and southeastern parts of the basin showed areas of light to moderate drought. By July, extreme drought

conditions expanded across central and eastern zones, affecting over 60% of the region. August presented a broader spread of moderate drought, while September marked the peak of drought intensity, with widespread severe conditions observed, especially in the northern and central areas. During October, drought persisted but shifted slightly in spatial extent, while November saw a reduction in severity across southern parts of the basin. Overall, the RF-based CDI-6 results demonstrated detailed spatial resolution and strong agreement with station-based SPEI-6 data, offering a reliable approach for drought monitoring at multiple time scales.

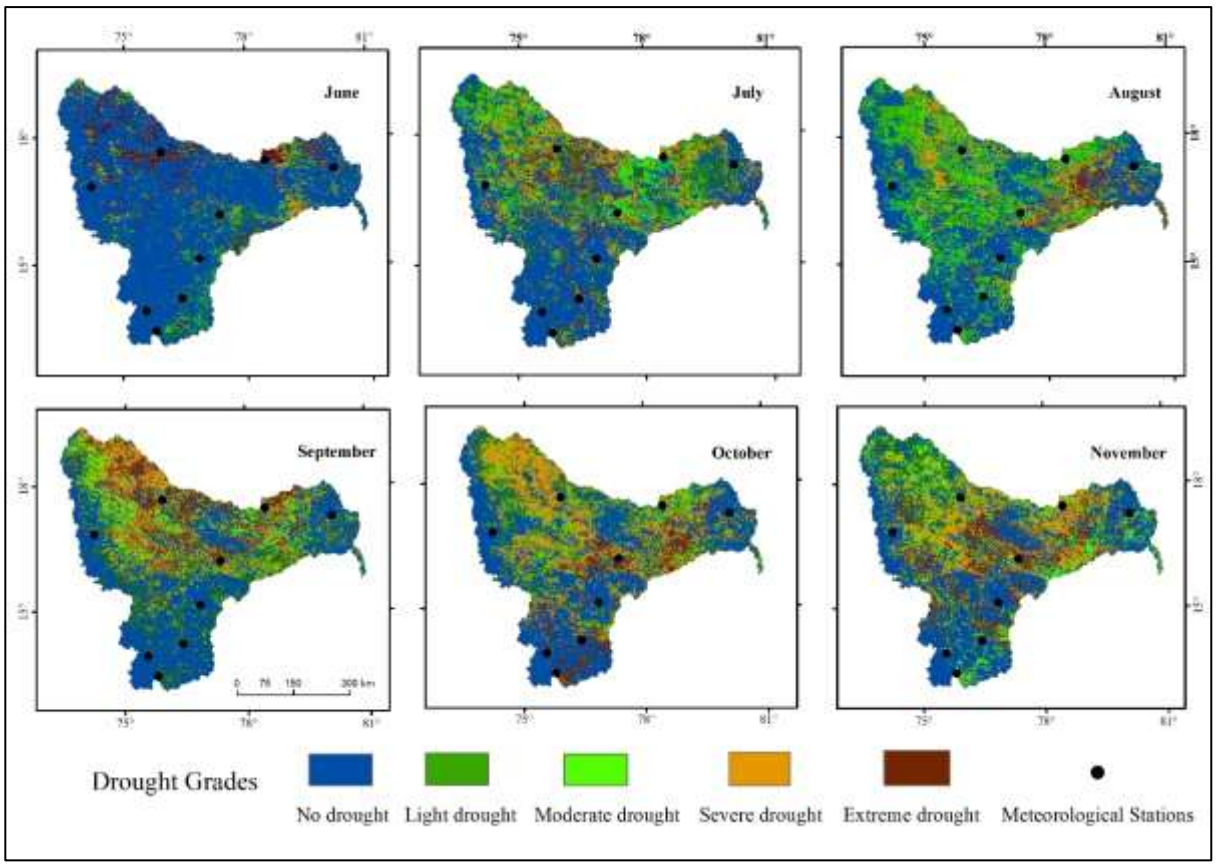

Figure- 10: *(June to November) are spatial distribution of CDI-6 from the Random Forest (RF) Model with station drought distribution during June to November 2021.*

In this study, the XGBoost model was utilized to develop a drought monitoring system for the Krishna River Basin, focusing on the period from June to November 2021. After comparative evaluation, SPEI-6 emerged as the most effective index for capturing severe and extreme drought events. Accordingly, the CDI-6 spatial distribution produced by the XGBoost model was compared against interpolated station-based SPEI-6 values to assess the accuracy and reliability of the model in identifying drought conditions. A visual comparison revealed a high degree of spatial agreement between CDI-6 outputs and station observations across various drought intensities. In June, large portions of the basin, especially the western and southern regions, showed little to no drought, while moderate drought appeared in scattered areas. By July, drought conditions intensified in the northern and eastern regions, with the spread of moderate to severe drought. During August, widespread moderate and severe drought conditions became evident, especially in the central and northern zones. September showed the highest severity, with extreme drought affecting vast areas in the northern and western parts of the basin. In October, the drought persisted with a slight shift towards the northeast, and by November, while southern areas showed

signs of recovery, central and northern parts remained under moderate to severe drought stress. Overall, the spatial distribution generated by the XGBoost model was consistent with station-based observations and provided detailed drought monitoring outputs, surpassing traditional interpolation methods in spatial accuracy.

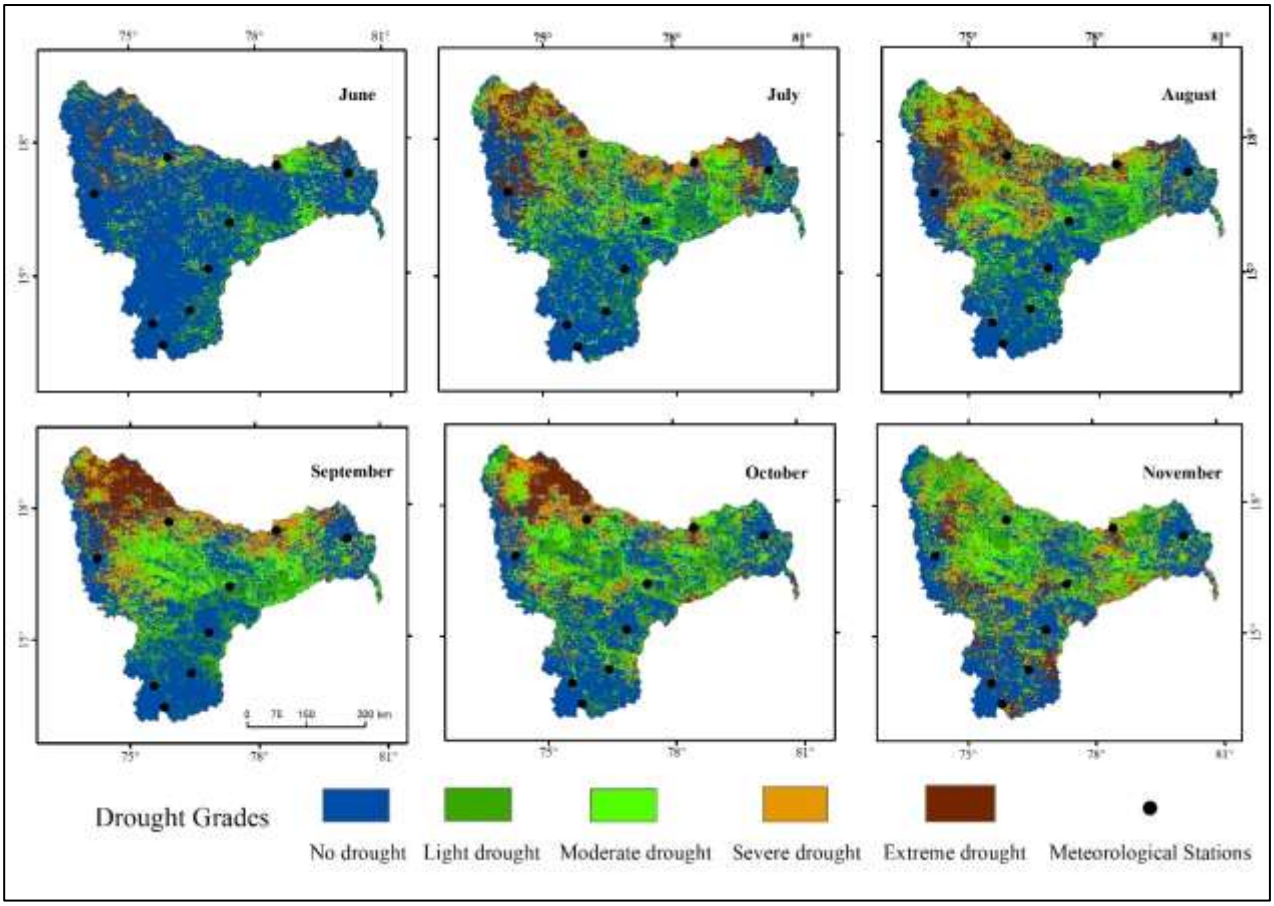

Figure- 11: *(June to November) are spatial distribution of CDI-6 from the XGBoost Model with station drought distribution during June to November 2021.*

In this study, the Long Short-Term Memory (LSTM) deep learning model was employed to build a drought monitoring system for the Krishna River Basin, covering the monsoon to post-monsoon period from June to November 2021. Among various time scales, SPEI-6 was found to be most effective in identifying severe to extreme drought events. Therefore, the spatial outputs of CDI-6, generated using the LSTM model, were compared with interpolated SPEI-6 station-based data to evaluate the spatial accuracy of drought detection. The comparison demonstrated a high level of agreement between LSTM-derived CDI-6 patterns and ground-based SPEI observations across most months. In June, much of the basin, particularly the central and western regions, experienced severe to extreme drought conditions. July showed a significant shift, with drought severity easing in the southern parts while persisting in the north and northeast. August marked further improvement in central zones, though severe drought remained in the east. By September, drought conditions intensified again, especially in the northern and western regions, where extreme drought was widespread. October revealed continued drought, with southern regions facing the most intense conditions. In November, extreme drought dominated the southern and southeastern areas,

while northern parts showed partial recovery. The LSTM model produced detailed spatial patterns of drought that closely reflected the observed severity levels, offering a strong alternative to traditional interpolation methods for operational drought monitoring.

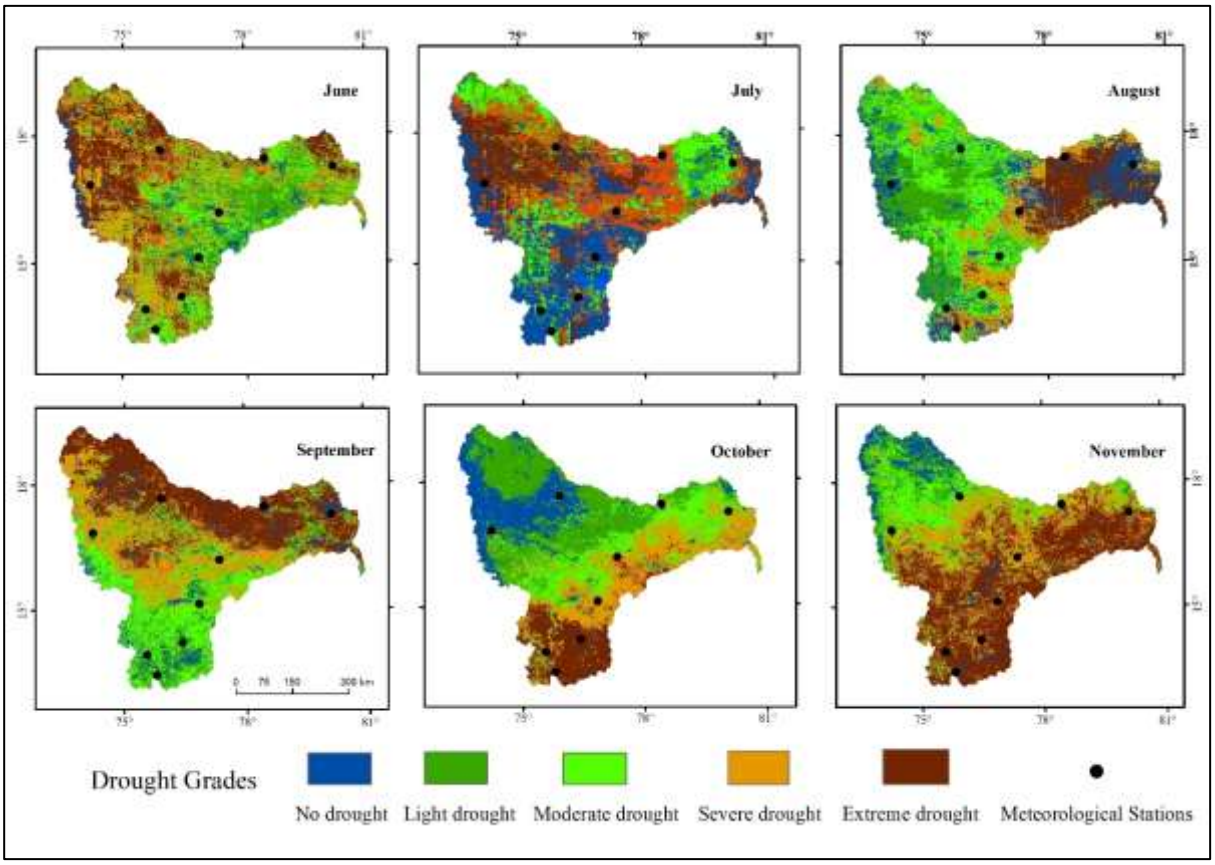

Figure- 12: *(June to November) are spatial distribution of CDI-6 from the LSTM Model with station drought distribution during June to November 2021.*

In this study, ConvLSTM was used to construct a drought monitoring model to monitor and classify drought from June to November in the Krishna Basin. After a comparative analysis, the SPEI-6 output outperformed other scales of SPEI in characterizing severe and extreme drought. Therefore, the CDI-6 Spatial distribution raster data and interpolated station SPEI-6 data were selected to evaluate the accuracy of CDI-6 spatial distribution in monitoring drought expressed The CDI-6 Spatial distribution and SPEI-6 observations at the actual station remained largely consistent. In June 2021, the western and southeastern regions of the Krishna Basin experienced light to moderate drought conditions. In July, extreme drought expanded across the basin, affecting more than 60% of the area, especially in central and eastern parts. By August, the drought trend began to ease in the northeastern and central zones. In September, the drought impact shifted westward, while the central basin showed moderate recovery. In October, further rainfall caused a significant reduction in drought severity, with light and no drought covering the largest areas. By November, most of the basin had recovered from severe drought, though small regions in the south and west still experienced severe to extreme drought conditions. Overall, the spatial distribution of CDI-6 from the ConvLSTM model was generally consistent with the drought severity derived from SPEI-6 observation, and the monitoring results were more spatially detailed than the interpolated station-based outcomes.

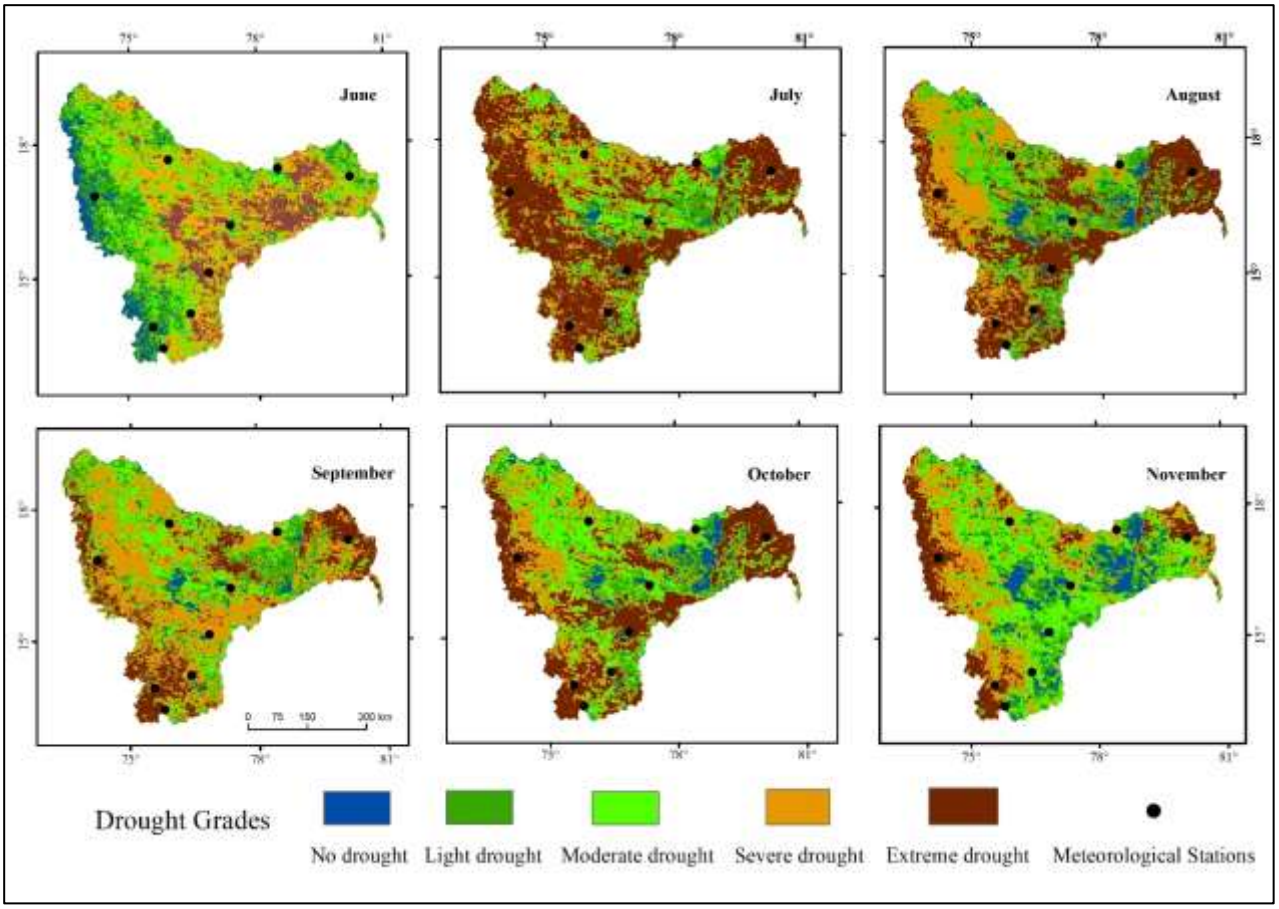

Figure- 13: *(June to November) are spatial distribution of CDI-6 from the ConvLSTM Model with station drought distribution during June to November 2021.*

4.6 Relative Importance of Differencing Influencing Factors on Simulation Results:

Drought is affected by multiple environmental factors. To analyses the influence of each variable on the drought monitoring results, this study used different indicators as independent variables in the model. The average reduction in accuracy was applied as a standard to determine the relative importance of each factor, and the results are shown in Table 10. For CDI-1, TCI had the highest influence (32.86), followed closely by ET (31.21) and VHI (26.81). This indicates that temperature and vegetation health were major contributions to the short-term drought model. PCI, SMCI and VCI had smaller contributions, with VCI having the least influence (1.38). in the CDI-3 model, TCI remained the most important factor (24.26_, followed by ET (23.88) and VCI (18.18). SMCI and PCI also had notable impacts, while VCI (1.20) showed the lowest contribution. For CDI-6, which reflects long-term drought conditions, ET (24.63), VHI (15.89), and TCI (14.48) were the top contributors. SMCI (15.53) and PCI (13.75) also played important roles. VCI had the lowest relative importance (0.76) in the long-term model. Overall, ET, TCI, and VHI were consistently the most influential variables across the models, suggesting that evapotranspiration and temperature-related factors are key in drought simulation. VCI had the lowest impact, especially in long-term drought analysis. This may be due to limitations in the vegetation index data or its lower responsiveness to prolonged drought stress in the Krishna River Basin.

Table- 10: *ConvLSTM CDI Relative importance of factors for drought assessment.*

Impact Factors	Relative Importance (%)		
	CDI-1	**CDI-3**	**CDI-6**
VCI	1.38	1.2	0.76
TCI	32.86	24.26	14.48
VHI	26.81	18.18	15.89
PCI	14.79	14.17	13.75
SMCI	13.92	15.76	15.53
ET	31.21	23.88	24.63

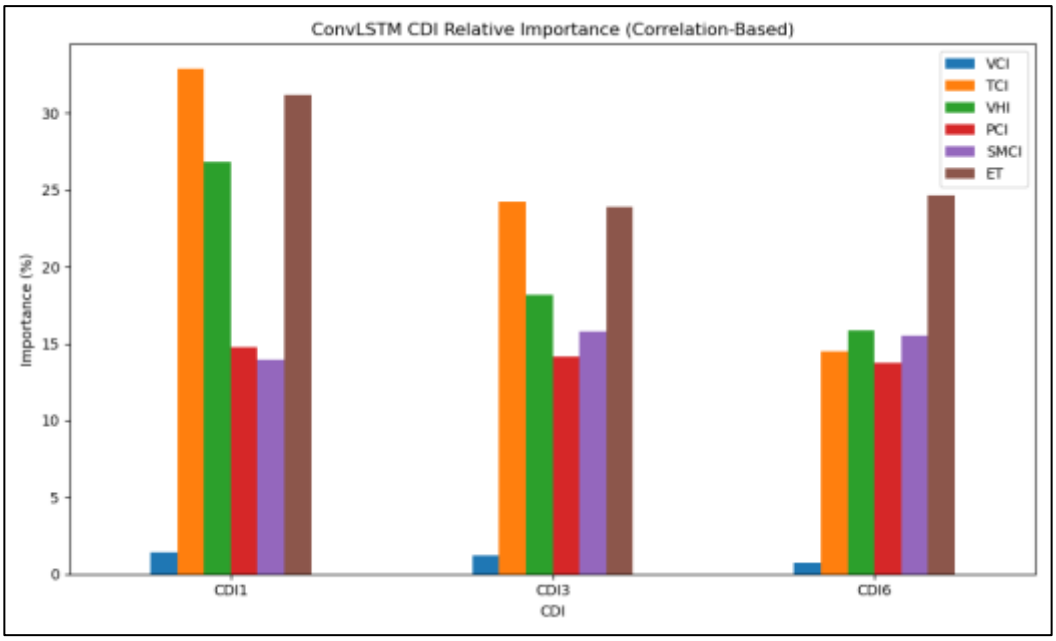

Figure - 14: *ConvLSTM CDI Relative importance of factors for drought assessment.*

5. DISCUSSION:

In this study, four distinct models—ConvLSTM, LSTM, XGBoost, and Random Forest (RF)—were developed and evaluated for drought monitoring in the Krishna River Basin using multi-source remote sensing and meteorological data to generate a Comprehensive Drought Index (CDI). Each model demonstrated strengths and limitations in capturing spatial and temporal drought dynamics across various time scales (CDI-1, CDI-3, and CDI-6).

The ConvLSTM model provided the most detailed and temporally consistent drought detection results. Its ability to simultaneously learn spatial features and temporal dependencies allowed it to accurately capture complex relationships among variables such as temperature, vegetation, precipitation, and evapotranspiration. However, ConvLSTM was computationally demanding and required extensive tuning, and its interpretability was limited due to the “black-box” nature of deep learning models. Despite this, feature importance analysis revealed that ET and TCI were dominant

contributors to CDI across all time scales, while VCI had minimal influence on longer drought durations (CDI-6).

The LSTM model, while less spatially complex than ConvLSTM, also performed well in modeling temporal drought patterns. It effectively captured trends in drought progression, particularly for medium and short-term droughts. However, it was less precise in spatial pattern detection compared to ConvLSTM and showed some lag in responsiveness to drought onset and recovery in peripheral regions of the basin.

XGBoost, a gradient-boosted decision tree model, achieved high accuracy and outperformed traditional models in terms of processing efficiency. It produced relatively smooth spatial outputs and captured severe drought zones effectively. The model was easier to interpret compared to deep learning models and required less computational power, making it suitable for rapid assessment. Nonetheless, its ability to handle temporal dependencies was limited, relying heavily on engineered temporal features.

The Random Forest model provided robust drought classification with strong agreement with station-based SPEI data. It performed well in identifying general drought trends and spatial coverage, though it occasionally missed finer temporal transitions in drought severity. RF was the most computationally efficient among the models and less sensitive to data noise, but lacked the depth to fully capture multi-variable interactions over time.

Across all models, some limitations were observed. The varying spatial resolution of input datasets introduced uncertainties in prediction accuracy. The use of monthly time steps limited the ability to detect rapid-onset droughts. Additionally, the lack of high-resolution, long-term soil moisture data and the uneven distribution of meteorological stations may have affected ground-truth validation. Land cover diversity in the Krishna Basin (agriculture, forest, urban) further contributed to spatial variation in model performance. Moreover, some relevant variables such as elevation, albedo, and soil water-holding capacity were not included in the current models but will be incorporated in future work to improve drought characterization.

Overall, ConvLSTM excelled in spatiotemporal drought tracking, LSTM showed strong temporal learning, XGBoost balanced performance with efficiency, and RF provided reliable baseline classification with minimal computational cost. Each model offers valuable insights for integrated drought monitoring, and their complementary strengths suggest potential for hybrid model development in future studies.

6. SUMMARY AND CONCLUSION:

Drought is a complex and evolving natural hazard that significantly impacts agriculture, ecosystems, and water resources. Effective monitoring and prediction of drought are crucial for early warning, risk mitigation, and sustainable resource management. This study aimed to develop and evaluate an integrated drought monitoring framework for the Krishna River Basin by applying four advanced machine learning and deep learning techniques: ConvLSTM, LSTM, XGBoost, and Random Forest. These models utilized a combination of remote sensing-based indices (VCI, TCI, SMCI, VHI, ET, PCI) and meteorological station data to generate the Comprehensive Drought Index (CDI) at multiple time scales—CDI-1, CDI-3, and CDI-6.

The ConvLSTM model demonstrated the strongest capability in capturing both spatial and temporal drought patterns. By incorporating convolutional layers, it successfully identified spatial features along with time series dynamics, leading to highly accurate and detailed drought classification maps. The model showed high agreement with station-based SPEI data, achieving over 80% classification accuracy across most drought categories, and strong correlation coefficients above 0.5 ($p < 0.01$). CDI-1 from ConvLSTM also aligned well with GLDAS-derived soil moisture, confirming its effectiveness for short-term agricultural drought assessment. However, the model's complexity, high computational requirements, and reduced interpretability present challenges for real-time or operational deployment without sufficient infrastructure.

The LSTM model, while lacking spatial filtering capabilities, was effective in modeling time series drought evolution. It performed particularly well for short- and mid-term drought trends, although its spatial predictions were slightly less precise than ConvLSTM. Still, it offers a balance between model complexity and temporal accuracy, making it a viable choice when resources are limited.

In contrast, XGBoost, a gradient boosting decision tree model, provided high accuracy and efficiency. It generated detailed spatial outputs, effectively captured severe drought zones, and required significantly less computational time than deep learning models. Moreover, its interpretability and ease of tuning make it practical for real-world applications. However, its performance was somewhat dependent on well-engineered input features to represent temporal variation.

The Random Forest model, while the simplest of the four, produced consistent and reliable results. It successfully classified general drought trends and spatial distribution, closely matching SPEI data. Though less sensitive to finer spatiotemporal variations, it was the most efficient and stable model, offering a strong baseline for drought assessment.

Across all models, ET and TCI emerged as the most influential variables, highlighting the importance of surface temperature and evapotranspiration in determining drought severity in the Krishna Basin. In contrast, VCI showed lower importance, particularly for long-term drought (CDI-6), suggesting that vegetation response alone is less indicative of prolonged drought stress.

Some challenges were identified during the study. The use of multi-source datasets with varying spatial resolutions introduced potential biases. In addition, long-term high-resolution soil moisture data were limited, and station-based validation was affected by uneven distribution and local climatic variability. The models were trained on monthly data, which may not capture rapid-onset droughts or sub-monthly fluctuations. Also, variables like elevation, land use, albedo, and soil properties were not included but should be integrated in future research for enhanced accuracy.

In conclusion, this research demonstrates that deep learning and ensemble machine learning models can significantly improve the accuracy and spatial resolution of drought monitoring when compared to traditional approaches. ConvLSTM and XGBoost in particular offer promising capabilities for developing real-time, data-driven early warning systems. The proposed framework contributes to improving drought risk management and supports decision-making in agriculture, water allocation, and climate adaptation planning. Future work should focus on integrating real-time data, higher spatial resolution variables, and expanding the models to cover additional environmental factors to build a more comprehensive and scalable drought monitoring system.

7. REFERENCE:

1. P. Sandeep, G.P. Obi Reddy, R. Jegankumar, K.C. Arun Kumar,2020. Monitoring of agricultural drought in semi-arid ecosystem of Peninsular India through indices derived from time-series CHIRPS and MODIS datasets. (https://doi.org/10.1016/j.ecolind.2020.107033).

2. Safwan Mohammed, Sana Arshad, Firas Alsilibe, Muhammad Farhan Ul Moazzam, Bashar Bashir, Foyez Ahmed Prodhang, Abdullah Alsalman, Attila Vad, Tam´ as Ratonyia, Endre Hars´ anyi, 2024. Utilizing machine learning and CMIP6 projections for short-term agricultural drought monitoring in central Europe (1900–2100). (https://doi.org/10.1016/j.jhydrol.2024.130968).

3. K. Niranjan Kumar, M. Rajeevan, D.S. Pai, A.K. Srivastava, B. Preethi, 2013.On the observed variability of monsoon droughts over India. (http://dx.doi.org/10.1016/j.wace.2013.07.006).

4. Xin Xiao, Wenting Minga, Xuan Luo, Luyi Yang, Meng Li, Pengwu Yang, Xuan Jia, Yungang Li, 2024. Leveraging multisource data for accurate agricultural drought monitoring: A hybrid deep learning model. (https://doi.org/10.1016/j.agwat.2024.108692).

5. Humberto A. Barbosa, Catarina O. Buriti and T. V. Lakshmi Kumar, 2024. Deep Learning for Flash Drought Detection: A Case Study in Northeastern Brazil. (https://doi.org/10.3390/atmos15070761).

6. Chirawat Wattanapanich, Thanongsak Imjai, Fetih Kefyalew, Pakjira Aosai, Reyes Garcia, Suseela Vappangi and Takafumi Noguchi, 2024. Integration of Internet of Things (IoT) and Machine Learning for Management of Ground Water Banks in Drought-prone Areas: A Case Study from Imjai Organic Garden, Thailand. (https://dx.doi.org/10.30919/es1248).

7. Junwei Zhou, Yanguo Fan, Qingchun Guan and Guangyue Feng, 2024. Research on Drought Monitoring Based on Deep Learning: ACaseStudy of the Huang-Huai-Hai Region in China. (https://doi.org/10.3390/land13050615).

8. Yuchi Wang, Jiahe Cui and CunzhuLiang, Bailing Miao, Zhiyong Li, Yongli Wang, Chengzhen Jia, 2024. Evaluating Performance of Multiple Machine Learning Models for Drought Monitoring: A Case Study of Typical Grassland in Inner Mongolia. (https://doi.org/10.3390/land13060754).

9. Yonghong Zhang, Donglin Xie, Wei Tian, Huajun Zhao, Sutong Geng, Huanyu Lu, Guangyi Ma, Jie Huang and Kenny Thiam Choy Lim Kam Sian, 2023. Construction of an Integrated Drought Monitoring Model Based on Deep Learning Algorithms. (https://doi.org/10.3390/rs15030667).

10. Tariq Ali, Saif Ur Rehman, Shamshair Ali, Khalid Mahmoo, Silvia Aparicio Obregon, Rubén Calderón Iglesias, Tahir Khurshaid & Imran Ashraf, 2024. Smart agriculture: utilizing machine learning and deep learning for drought stress identification in crops. (https://doi.org/10.1038/s41598-024-74127-8).

11. Yashvita Tamrakar, I. C. Das, Swati Sharma, 2024. Machine learning for improved drought forecasting in Chhattisgarh India: a statistical evaluation. (https://doi.org/10.1007/s44288-024-00089-z).

12. Xiaohui Yang, Feng Gao, Hongwei Yuan and Xiuqing Cao, 2024. Integrated UAV and Satellite Multi-Spectral for Agricultural Drought Monitoring of Winter Wheat in the Seedling Stage. (https://doi.org/10.3390/s24175715).

13. Song, Y.; Fang, S.; Yang, Z.; Shen, S, 2018. Drought indices based on MODIS data compared over a maize-growing season in Songliao Plain, China. (https://doi.org/10.1117/1.JRS.12.046003).

14. Alnaanah, M.; Wahdow, M.; Alrashdan, M., 2022. CNN models for EEG motor imagery signal classification. (CNN models for EEG motor imagery signal classification | Signal, Image and Video Processing).

15. Runping Shen, Anqi Huang ", Bolun Li ", Jia Guo b, 2019. Construction of a drought monitoring model using deep learning based on multi-source remote sensing data. (https://doi.org/10.1016/j.jag.2019.03.006).